

## Experimentally designed optimized conditions for catalytic performance of nanostructured RuO<sub>2</sub> in Biginelli reaction

F. Soleimani, M. Behzad\*, M. Salehi

Department of chemistry, Semnan University, Semnan 35351-19111, Iran

### Article history:

Received 08/09/2015

Accepted 02/11/2015

Published online 01/12/2015

### Keywords:

Hydrothermal

Ruthenium(IV) oxide

Biginelli

Experimental design

Nanocatalyst

### \*Corresponding author:

Mahdi Behzad

mbehzad@semnan.ac.ir;

mahdibehzad@gmail.com

Phone: +98-23 33383195

### Abstract

Nanostructured RuO<sub>2</sub> powders were synthesized via a hydrothermal method at 180 °C for 12 h using 1 and 2 M NaOH aqueous solutions. The structure of the obtained nanomaterials was investigated by powder X-ray diffraction (PXRD) technique. The morphology the obtained materials were studied by field emission scanning electron microscope (FESEM). The technique showed that with changing the reaction rout, the homogeneity of the size and morphology of the synthesized nanomaterials were changed. It was found that the morphology of the obtained materials were spherical particles using 2 M NaOH aqueous solution. Catalytic performance of the synthesized nanomaterials was investigated in Biginelli reactions for the one-pot synthesis of 3,4-dihydropyrimidin-2(1H)-ones (DHPMs) using Benzaldehyde derivatives, urea and ethylacetoacetate as raw materials. Experimental design method was used to obtain optimized reaction conditions. It was found that the optimized conditions were 0.028 g of catalyst, 110 °C reaction temperature and 66 min reaction time.

2015 JNS All rights reserved

## 1. Introduction

Anhydrous Ruthenium oxide (RuO<sub>2</sub>) has versatile functionality. It has been extensively used as catalyst in organic and inorganic reactions [1], as a dimensionally stable anode for chlorine generation for chloric-alkali industry [2], as electrocatalyst for oxygen and hydrogen production in water electrolysis [3], and as catalyst and electrode in super capacitors

[4-7]. There are various ways for synthesis ruthenium (IV) oxide including chemical vapor deposition [8], pyrolysis [9], electroplating and electro deposition [10], thermal decomposition [11], sol-gel process [6], electrostatic spray deposition [12], sputtering [13], hydrothermal [1], and so forth. In this work, a simple and straightforward hydrothermal process has been used to synthesis nanostructured RuO<sub>2</sub>. RuCl<sub>3</sub>.xH<sub>2</sub>O

and NaOH were used as raw materials. PXRD and FESEM techniques were used to characterize and analyze the properties of the synthesized RuO<sub>2</sub> nanoparticles. Cell parameter refinements were also performed. The catalytic performance of the synthesized nanomaterial was investigated in Biginelli reactions for the synthesis of 3,4-dihydropyrimidin-2-(1H)-ones (DHPMs). Several other metal oxides have been used as catalyst in Biginelli reactions e.g. Al supported Mo [14], ZnO [15], and TiO<sub>2</sub> [16], mesoporous aluminum silicate [17], Mg/MeOH [18], CeO<sub>2</sub> supported on poly (4-vinylpyridine-co-divinylbenzene) (PVP-DVB)/H<sub>2</sub>O [19] and so on. Several parameters affecting the reaction efficiency, including reaction temperature, time and the amount of the catalyst, were optimized by experimental design method using full factorial design coupled to response surface methodology (RSM) [20], based on central composite design (CCD) [21]. Excellent performance was achieved in the optimized conditions.

## 2. Experimental

### 2.1. General remarks

All chemicals were of analytical grade, obtained from commercial sources, and used without further purifications. Phase identifications were performed on a powder X-ray diffractometer D5000 (Siemens AG, Munich, Germany) using CuK $\alpha$  source. Cell parameter refinements were performed by celref software version 3 (Laboratoire des Matériaux et du Génie Physique de l'École Supérieure de Physique de Grenoble). The morphologies of the obtained materials were examined with a field emission scanning electron microscope (Hitachi FE-SEM model S-4160). The purity of the DHPMs was checked by thin layer chromatography (TLC) on glass plates coated with silica gel 60 F254 using n-hexane/ethyl acetate

mixture as mobile phase and melting point analysis on a thermoscientific 9100 apparatus.

### 2.2. Hydrothermal synthesis of RuO<sub>2</sub> nanocatalyst

In a typical experiment, 0.5 g (2.4 mmol) RuCl<sub>3</sub>.10H<sub>2</sub>O was dissolved in 1M (S<sub>1</sub>) or 2M (S<sub>2</sub>) NaOH aqueous solutions with heating and stirring at 90 °C for 20 min. The obtained solution was transferred into a 100 mL teflon-lined stainless steel autoclave and kept at 180 °C for 12 h. When the reaction was completed, the autoclave was immediately cooled down by water. The precipitate was then filtered and dried at 120 °C for 10 min to yield a black powder. Typical yields of about 0.25 g (75 %) were obtained.

### 2.3. General procedure for the synthesis of DHPMs

In a typical experiment, aldehyde (1 mmol), ethyl acetoacetate (1 mmol), urea (1.2 mmol) and catalytic amounts of RuO<sub>2</sub> (S<sub>2</sub>) were mixed and magnetically stirred in a round-bottom flask under solvent free conditions [22]. The reaction progress was checked by thin layer chromatography (TLC) [6:4 hexane:ethylacetate]. After completion of the reaction, the solid product was washed with deionized water to separate the unreacted raw materials. Then, the precipitation was gathered and dissolved in ethanol to separate the solid catalyst. The filtrate was evaporated to dryness by a rotary evaporator to afford the crude product which was then recrystallized in ethanol to afford crystals of the pure DHPMs.

## 3. Results and discussions

### 3.1. Characterization

The X-ray diffraction patterns of the RuO<sub>2</sub> nanomaterials are shown in figure 1, where **a** shows (S<sub>1</sub>), and **b** (S<sub>2</sub>). The XRD patterns showed that the synthesized nanomaterials were crystallized in a

tetragonal crystal structure, with space group of  $P4_2/mnm$  (JCPDS 40-1290). The lattice parameters were found as  $a = b = 4.4994 \text{ \AA}$ ,  $c = 3.1071 \text{ \AA}$  with  $\alpha = \beta = \gamma = 90$  [23, 24]. For the most intense diffraction line (hkl: 101), a diffraction line shift of  $\Delta 2\theta = 0.27^\circ$  ( $35.03^\circ$  ( $S_2$ ) –  $35.30^\circ$  ( $S_1$ )) and  $\Delta d = 0.03 \text{ \AA}$  ( $2.56 \text{ \AA}$  ( $S_1$ ) –  $2.530 \text{ \AA}$  ( $S_2$ )) were calculated via Bragg's law. Table 1 shows the cell parameter refinement data for  $S_1$  and  $S_2$ . It was found that by changing the reaction conditions, the volume of the unit cell was decreased. So there is a contraction in the unit cell with increasing NaOH concentration for the synthesis of  $\text{RuO}_2$ .

**Table 1.** Cell parameters of samples 1 and 2 and tabulated values for  $\text{RuO}_2$ . SD is the standard deviations.

Sample	a (SD)	b (SD)	c (SD)	Volume (SD)
(JCPDS 40-1290)	4.4994	4.4994	3.1071	62.90
$S_1$	4.5514 (0.0377)	4.5514 (0.000)	3.0476 (0.0123)	63.13 (0.581)
$S_2$	4.4982 (0.0045)	4.4982 (0.000)	3.1066 (0.0012)	62.86 (0.067)

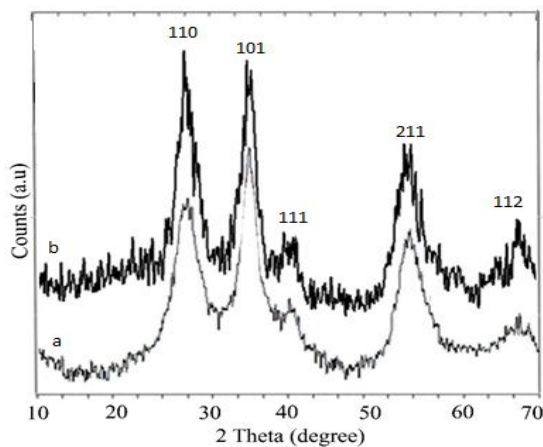


**Fig. 1.** PXRD patterns of (a)  $S_1$  and (b)  $S_2$ .

Figures 2 and 3 show the FESEM images of  $S_1$  and  $S_2$ , respectively. Figure 2 shows that the synthesized nanomaterial had sphere-like morphology and the diameter size of the synthesized nanomaterials were in the range of about 50-70 nm. However, the figure shows that there were large bulks in the sample too. On the other hand, analysis of figure 3 showed that the synthesized nanomaterials' sizes and morphologies were nearly homogeneous. It was found that the materials were in sphere-like structure and there were no bulks in the sample. Figure 3 shows that the sizes of the materials were in the range of about 20-60 nm.

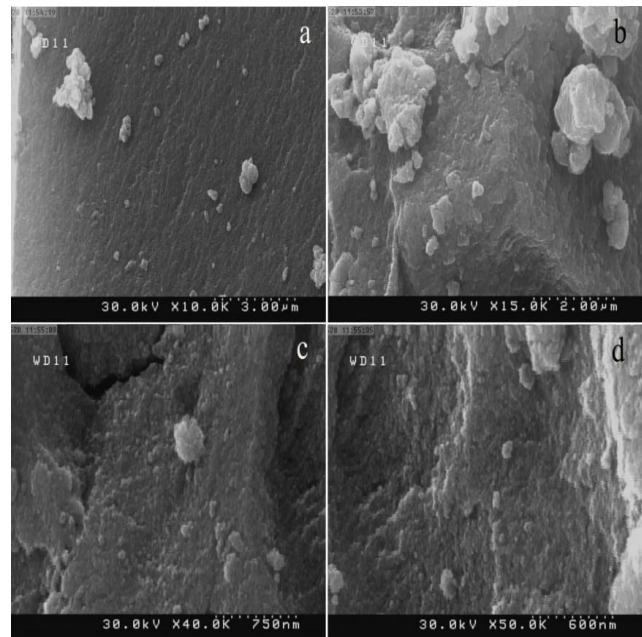


**Fig. 2.** FESEM images of  $S_1$ .

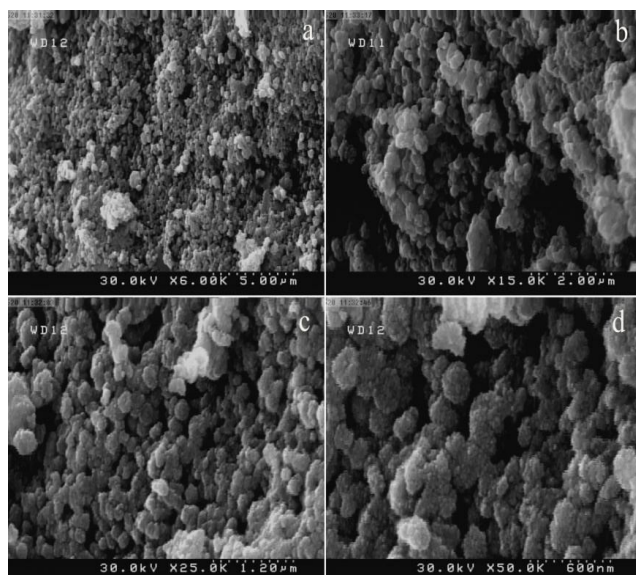


Fig. 3. FESEM images of  $S_2$ .

### 3.2. Catalytic studies

#### 3.2.1. Central Composite design and optimal condition in Biginelli reactions

Central composite design (CCD), proposed by Box and Wilson, is one of the most common methods in response surface methodology (RSM) for fitting a second order (quadratic) model [25, 26]. In this method, each factor is set at five levels ( $-\alpha$ ,  $-1$ ,  $0$ ,  $1$ ,  $\alpha$ ) except for  $\alpha=1$ . A CCD is composed of  $N$  experiment which has the following distribution:

1-  $n_F$  experiments of a two-level factorial design. These are the only points that are applied to calculate two-factor interactions.

2-  $2k$  experiments of a ‘star’ design, which are not used for the estimation of interaction terms.

3.  $n_C$  center points which provide random error value and also are applied to estimate all of the terms of a quadratic model.

So, the number of experiments ( $N$ ) is as follows:

$$N = 2^k + 2k + C_0 \quad (\text{Eqn. 1})$$

Where  $k$  is the number of factors.  $2^k$ ,  $2k$  and  $C_0$  are factorial, star and central points, respectively [25]. In this study, the amount of the catalyst ( $X_1$ ), temperature ( $X_2$ ) and time of the reaction ( $X_3$ ) which were the three effective factors for Biginelli reaction, were designed based on CCD as presented in table 2. This design was consisted of twenty experiments including six center points and they were conducted randomly in three days. All the experiments and the design are listed in table 3.

Table 2. Factors and levels applied in the CCD design.

Factors	Symbol	Levels				
		$-\alpha$	$-1$	$0$	$1$	$\alpha$
The amount of the catalyst (g)	$X_1$	0.005	0.014	0.034	0.041	0.050
Temperature ( $^{\circ}\text{C}$ )	$X_2$	40	56	75	104	120
Time (min)	$X_3$	10	24	43	65	80

Table 3. Design matrix and responses for the CCD design.

Catalyst amount (g)	Temp (°C)	Time (min)	Yield (%)
<b>day1</b>			
0.041	56	66	50
0.014	56	24	32
0.034	75	43	66
0.014	104	66	89
0.041	104	24	82
0.03	75	43	70
<b>day2</b>			
0.041	56	24	65
0.014	56	66	68
0.034	75	43	66
0.028	75	43	60
0.014	104	24	47
0.041	104	66	88
<b>day3</b>			
0.028	120	45	100
0.034	75	43	58
0.050	80	45	63
0.028	80	10	39
0.028	80	80	75
0.034	75	43	65
0.028	40	45	58
0.005	80	45	38

RSM is a collection of mathematical and statistical methods, which fits N experiments response of the CCD according to the quadratic equation 2:

$$Y = \beta_0 + \sum_{i=1}^k \beta_i x_i + \sum_{i=1}^k \beta_{ii} x_i^2 + \sum_{i < j} \beta_{ij} x_i x_j +$$

$\epsilon$

(Eqn. 2)

That  $\beta$ s are coefficients which in the sentences with first order show main effects, in the terms with second

order represent quadratic effects and in the statements with multiplication factors are interaction effects. Y is the response at each experiment, here it is the percent yield of the reaction;  $x_i$ s are the independent factors. In RSM, by conducting a regression analysis, the coefficients are calculated. In turn, analysis of variance (ANOVA) [21, 27], is used to verify the adequacy of the model. Analysis of the CCD data, presented in table 3, by RSM based on equation 2, described the relationship between the factors and the yield of the reaction, Y, as shown by equation 3, in which  $X_1$ ,  $X_2$  and  $X_3$  are and the same as the coded factors introduced in table 3.

$$Y = 64.79 + 6.66 X_1 + 11.77 X_2 + 9.43 X_3 + 2.35X_1X_2 - 10.76X_1X_3 + 3.31 X_2X_3 - 4.35 X_1^2 + 5.73 X_2^2 - 2.05 X_3^2$$

The ANOVA of the above models has been presented in table 4. P-value smaller than 0.1, provides a poof of its significance at confidence level (90%). As it could be seen from table 4, all the parameters had the p-value smaller than 0.05, a fact which showed that all factors, interaction and quadratic effects except for  $X_1X_2$  were significant. The p-value of the whole model is even less than 0.0001, which highly proves the signification in the applied quadratic model. The p-value of lack of fit

was much more than 0.05, i.e. 0.561, also confirmed the models' high significance. Moreover, the coefficient of determination (the R-square, adjusted-R-square) were indicators of the quality of the fit. In this case,  $R^2$  equaled 0.9780 indicating a high degree of correlation between the response and the independent factors. Adjusted regression coefficient ( $R^2$ -adj = 0.9532) also showed the significance of the applied model.  $R^2$ -pred is a parameter whose value shows the prediction ability of the fitted model. Here,  $R^2$ -pred was 0.838 which shows the high prediction power of the model.

**Table 4.** Analysis of variance for suggested quadratic model [28].

Source	DF	SS	F	P
Block	2	52.78		
Model	6	5721.36	39.48	<0.0001
$X_1$	1	606.41	37.66	0.0003
$X_2$	1	1912.64	118.80	< 0.0001
$X_3$	1	1227.76	76.26	< 0.0001
$X_1 X_2$	1	45.16	2.81	0.1325
$X_1 X_3$	1	946.05	58.76	< 0.0001
$X_2 X_3$	1	91.11	5.66	0.0446
$X_1^2$	1	221.51	13.76	0.0060
$X_2^2$	1	431.14	26.78	0.0008
$X_3^2$	1	56.61	3.52	0.0976
Residual	8	128.80		
Lack-of-fit	5	78.30	0.93	0.5612
Pure error	3	50.50		
Total	19	5902.95		

To depict the effects in the above model, the three-dimensional (3D) response surfaces plots of the

response, based on equation (3), when one factor value was fixed at centre level and the other two were varied are shown in figures 4-6. The curvature of the plot showed that there was interaction between the factors. It meant that the

factors influenced the response interactively and not independently. The goal of the optimization was to find optimal conditions in which the yield of the reaction was maximized. These conditions were achieved by maximizing the equation (3) when the amount of the catalyst was 0.028 g, at 110 °C reaction temperatures, and 66 min reaction times.

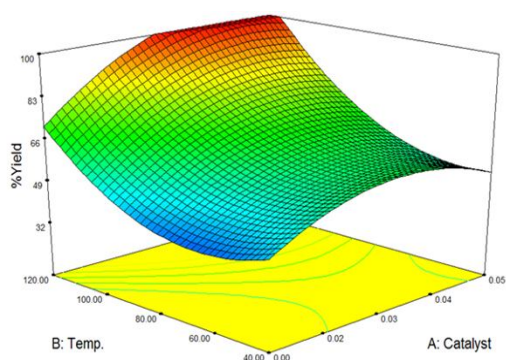


**Fig. 4.** 3D plot of the response surface of Biginelli reaction yield percent vs. the amount of the catalyst and temperature at fix reaction time (45 min).

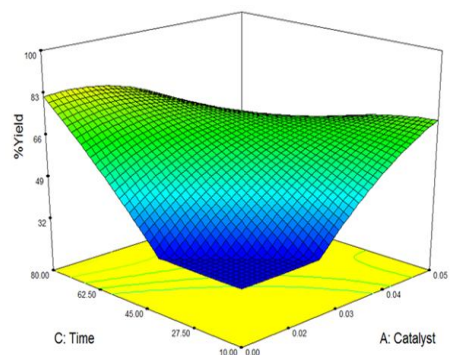


**Fig. 5.** 3D plot of the response surface of Biginelli reaction yield percent vs. the amount of the catalyst and time at fixed reaction temperature (80 °C).

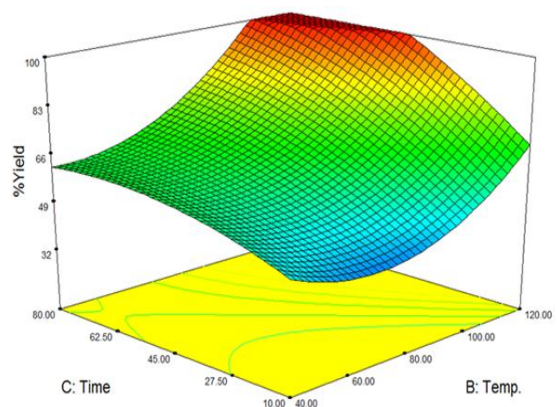
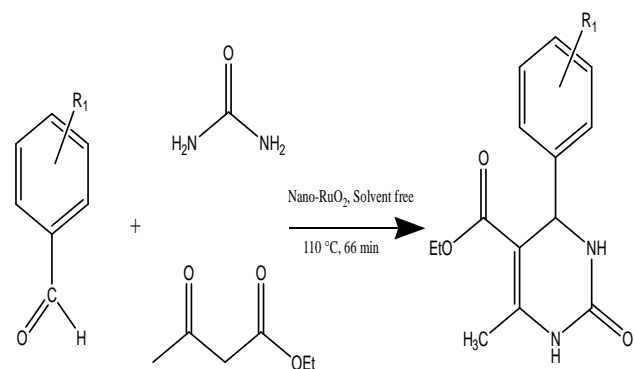


**Fig. 6.** 3D plot of the response surface of Biginelli reaction yield percent vs. the time and temperature at fix amount of the catalyst (0.034 g).

The optimized parameters from the previous section (0.028 g, 110 °C and 66 min) were used for the synthesis of other SHPMs and the results are collected in table 5. Scheme 1 shows a summary of the reaction pathway. As could be seen from table 5, excellent performance was achieved at the optimized conditions.



**Scheme 1.** Schematic representation of the reaction pathway for the synthesis of DHPMs.

**Table 5.** Biginelli reactions using ethyl acetoacetate and urea with different benzaldehyde derivatives.

R <sub>1</sub>	Conversion (%)
H	98
4- Cl	99
2- Cl	90
4- Br	99
3- OCH <sub>3</sub>	58
4-OH	97
3-OH	100
3-NO <sub>2</sub>	97
3,4-O	85

To show the merit of the present work in comparison with reported results in the literature, we compared RuO<sub>2</sub> nanocatalyst results with reported catalysts in the synthesis of DHPMs (table 6). It is clear that RuO<sub>2</sub>

has shown a greater activity than some other heterogeneous catalysts.

**Table 6.** Comparison study of the catalytic ability of the synthesized RuO<sub>2</sub> with other catalysts.

Catalyst	R <sub>1</sub>	Catalyst amount	Conditions	Yield %	Time	Ref.
RuO <sub>2</sub>	H	2.25×10 <sup>-2</sup> mmol	solvent-free condition, 110°C	98	66 min	This work
	4- Cl			99		
	2- Cl			90		
Bi <sub>2</sub> O <sub>3</sub> /ZrO <sub>2</sub>	H	20 mol%	solvent-free conditions, 80-85 °C	85	120 min	[29]
	4- Cl			85	120 min	
	2- Cl			82	165 min	
ZrO <sub>2</sub> -Al <sub>2</sub> O <sub>3</sub> -Fe <sub>3</sub> O <sub>4</sub>	H	0.05 g	Ethanol, reflux, 140°C	82	300 min	[30]
	4- Cl			66		
	2- Cl			40		
Mo/γ - Al <sub>2</sub> O <sub>3</sub>	H	0.3 g	solvent-free conditions at 100 °C	80	60 min	[31]



ZnO	H	25 mol%	solvent-free conditions at 90 °C	92	50 min	[32]
	4-Cl			95		
Bi <sub>2</sub> V <sub>2</sub> O <sub>7</sub>	H	3.1 × 10 <sup>-2</sup> mmol	solvent-free conditions at 90 °C	89		[33]
	4-Cl			92		
	2-Cl			98		
Bi <sub>2</sub> Mn <sub>2</sub> O <sub>7</sub>	H	2.2 × 10 <sup>-2</sup> mmol	solvent-free conditions at 104 °C	96		[34]
	4-Cl			89		
	2-Cl			86		

#### 4. Conclusion

In summary, nanostructured crystalline RuO<sub>2</sub> was synthesized by a mild condition hydrothermal method. FESEM studies showed that the obtained nanomaterials had sphere-like structure. Cell parameter refinements were investigated.

The catalytic application of the synthesized nanomaterials was investigated in Biginelli reaction in solvent free conditions. It was found that RuO<sub>2</sub> nanomaterial had excellent efficiency in the synthesis of DHPMs. Optimized reaction conditions were obtained by experimental design method.

#### References

- [1] K. H. Chang, C. C. Hu, *Electrochem Solid-State Lett.* 7 (2004) 466-469.
- [2] S. Trasatti, *Electrochem Acta.* 36 (1991) 225-241.
- [3] J. Lipkowski, P. N. Ross, *The electrochemical novel materials*, VCH Publishers, 1994.
- [4] B. O. Park, C. D. Lokhande, H. S. Park, K. Jung, D.; O. S. Joo, *J. Power Sources.* 134 (2004) 148-152.
- [5] J. P. Zheng, P. J. Cygan, T. R. Jow, *J Electrochem Soc.* 142 (1995) 2699-2703.
- [6] W. Deng, X. Ji, Q. Chen, C. E. Banks, *RSC Adv.* 1 (2011) 1171-1178.
- [7] A. Burke, *Ultracapacitors.* 91 (2000) 37-50.
- [8] S. Pizzini, G. Buzzanca, C. Mari, L. Rossi, S. Torchio, *Mater Res Bull.* 7 (1972) 449.
- [9] V. D. Patake, C. D. Lokhande, *Appl Surf Sci.* 254 (2008) 2820-2824.
- [10] S. H. Lee, P. Liu, H. M. Cheong, C. E. Tracy, S. K. Deb, *Solid State Ionics.* 165 (2003) 217-221.
- [11] W. Dmowski, T. Egami, K. E. Swider-Lyons, C. T. Love, D. R. Rolison, *J Phys Chem B.* 106 (2002) 12677-12683.
- [12] I. H. Kim, K. B. Kim, *J. Electrochem Soc.* 153 (2006) A383-A389.
- [13] L. Krusin-Elbaum, M. Wittmer, *J Electrochem Soc.* 135 (1988) 2610-2614.
- [14] K. Kouachi, G. Lafaye, S. Pronier, L. Bennini, S. Menad, *J. Mol Catal A Chem.* 395 (2014) 210-216.
- [15] F. Tamaddon, S. Moradi, *J. Mol Catal A Chem.* 370 (2013) 117-122.
- [16] H. R. Memarain, Ranjbar, *M. J Mol Catal A Chem.* 356 (2012) 46-52.
- [17] D. Shobha, M. A. Chari, A. Mano, S. T. Selvan, K. Mukkanti, A. Vinu, *Tetrahedron.* 65 (2009) 10608-10611.

- [18] K. Singh, K. Singh, *Tetrahedron Lett.* 50 (2009) 2219-2221.
- [19] G. Sabitha, K. B. Reddy, J. S. Yadav, D. Shailaja, K. S. Sivudu, *Tetrahedron Lett.* 46 (2005) 8221-8224.
- [20] G. E. P. Box, N. R. Draper, *Empirical model-building and response surfaces.* Wiley, 1987.
- [21] R. H. Myers, D. C. Montgomery, *Response Surface Methodology: Process and Product Optimization Using Designed Experiments*, third ed., Wiley, 2002.
- [22] H. Valizadeh, A. Shockravi, *Heteroat Chem.* 20 (2009) 284-288.
- [23] J. H. Xu, T. Jarlborg; A. J. Freeman, *J Phys Rev.* 40 (1989) 7939.
- [24] J. Haines, J. M. Leger, *Phys Rev B.* 55 (1997) 11144.
- [25] G. E. Box, K. B. Wilson, *J R Stat Soc Series B.* 13 (1951) 1-45.
- [26] R. H. Myers, D. C. Montgomery, C. M. Anderson-Cook, *Response surface methodology: process and product optimization using designed experiments*, John Wiley and Sons. 2009.
- [27] R. H. Myers, D. C. Montgomery, G. G. Vining, C. M. Borrer, S. M. Kowalski, *J Qual Technol.* 36 (2004) 53.
- [28] R. Tauler, B. Walczak, S. D. Brown, *Comprehensive chemometrics: chemical and biochemical data analysis.* Elsevier, 2009.
- [29] V. C. Guguloth, G. Raju, M. Basude, S. Battu, *Int J Chem Anal Sci.* 5 (2014) 86-92.
- [30] A. Wang, X. Liu, Z. Su, H. Jing, *J Catal Sci Technol.* 4 (2014) 71-80.
- [31] S. L. Jain, V. V. D. N. Prasad, B. Sain, *Catal Commun.* 9 (2008) 499-503.
- [32] K. Pourshamsian, *Int J Nano Dimension.* 6 (2015) 99.
- [33] S. Khademinia, M. Behzad, H. S. Jahromi, *RSC Adv.*, 5 (2015) 24313.
- [34] S. Khademinia, M. Behzad, A. Alemi, M. Dolatyari, S. M. Sajjadi, *RSC Adv.* 5 (2015) 71109.